Nonlinear Transport and Heat Dissipation in Metallic Carbon Nanotubes

Marcelo A. Kuroda,[1,2] Andreas Cangellaris,[3] and Jean-Pierre Leburton[1,3]

[1]*Beckman Institute, University of Illinois at Urbana-Champaign, Illinois 61801, USA*

[2]*Department of Physics, University of Illinois at Urbana-Champaign, Illinois 61801, USA*

[3]*Department of Electrical and Computer Engineering, University of Illinois at Urbana-Champaign, Illinois 61801, USA*

(Received 8 July 2005; published 21 December 2005)

We show that the local temperature dependence of thermalized electron and phonon populations along metallic carbon nanotubes is the main reason behind the nonlinear transport characteristics in the high bias regime. Our model is based on the solution of the Boltzmann transport equation considering both optical and zone boundary phonon emission as well as absorption by charge carriers. It also assumes a local temperature along the nanotube, determined self-consistently with the heat transport equation. By using realistic transport parameters, our results not only reproduce experimental data for electronic transport but also provide a coherent interpretation of thermal breakdown under electric stress. In particular, electron and phonon thermalization prohibits ballistic transport in short nanotubes.

DOI: 10.1103/PhysRevLett.95.266803 PACS numbers: 73.63.Fg, 65.80.+n, 73.23.−b

Carbon nanotubes (CN) are one-dimensional (1D) nanostructures that have stimulated broad research interest because of their unique electrical versatility as semiconductors or metals, depending on their chirality [1]. From a technological viewpoint, their remarkable electrical and mechanical properties make them promising materials for applications in high performance nanoscale electronic and mechanical devices [2,3]. Among these properties, the interrelation between electronic and thermal transport in these quasi-1D structures is particularly interesting. Early experiments on nonlinear transport in metallic single walled nanotubes (m-SWNTs) using low resistance contacts revealed current saturation at the 25 μA level, a fact attributed to the onset of electron backscattering by high energy optical (OP) and zone boundary (ZB) phonons in the high bias regime [4]. More recently, series of independent high-field transport measurements on various length m-SWNTs demonstrated the absence of current saturation by achieving currents over 60 μA in short samples ($\lesssim$55 nm), which was interpreted as ballistic transport along the CN [5,6]. Thermal breakdown and burning under high electric stress were also observed in SWNT. In the interim, the electrical conductance of multiwalled nanotubes (MWNTs) under high bias has shown a steplike decrease caused by the successive burning of the CN outer shells [7,8]. In these experiments CNs burned unexpectedly at midlength under stress even on a substrate and on the presence of a back gate in a field effect device geometry [9]. Despite various attempts to model these systems [4–6], up to now no coherent interpretation has been proposed that reconciliates heat dissipation and electronic transport and describes thermal effects in m-CNs under electric stress.

In this Letter, we show that the nonlinear characteristics of metallic CNs find their origin in the nonhomogeneous Joule heating along the nanotube, which is caused by the thermalized distribution of electrons scattered by high energy phonons, even in short m-SWNT. We specifically show that Joule heating (temperature) is maximum at CN midlength. Moreover, owing to the 1D nature of the structure, Joule heating increases drastically at constant current with the CN length, resulting in thermal breakdown at lower electric fields than in shorter CNs. Our model is based on the Boltzmann transport equation with OP and ZB phonon scattering and solved self-consistently with the heat transfer equation, providing a coherent interpretation of electric and thermal transport in m-SWNTs, in agreement with experimental data [5,6]. In particular, we show that the high current level in short CNs is not due to ballistic transport but to reduced Joule heating.

We use the linear dispersion relation of electronic states around the Fermi level [$\epsilon(k) = \pm\hbar v_F k$] [10], where v_F is the Fermi velocity. Thus, the Boltzmann equation reads

$$v_F \partial_x f^\alpha(\epsilon) + \frac{eF}{\hbar}\partial_k f^\alpha(\epsilon) = C^\alpha_{\rm ph}(I, T). \qquad (1)$$

Here $f^\alpha(\epsilon)$, F, e, and $C_{\rm ph}$ are the distribution function for the α energy branch, the electric field, the electron charge, and the electron-phonon collision integral, respectively. The index α denotes the energy branches with positive (+) and negative (−) Fermi velocity in the first (1) and second valleys (2) of the m-CN. In metallic systems high electron density and strong intercarrier scattering thermalizes the electron distribution. We therefore assume that the electron distribution function $f^\alpha(\epsilon)$ obeys Fermi-Dirac statistics with a local electronic temperature $T_{\rm el}(x)$:

$$f^\alpha(\epsilon) = 1/\{1 + \exp[(\epsilon - \epsilon^\alpha_F)/k_B T_{\rm el}(x)]\}, \qquad (2)$$

where ϵ^α_F is the quasi Fermi level of branch α. As a result, the collision integral $C^\alpha_{\rm ph}$ also depends on the position. We neglect acoustic phonons that are only relevant in the low bias regime and consider the contribution of high density OP and ZB phonons [11,12] as playing a central role in energy dissipation in the high bias regime. As illustrated in

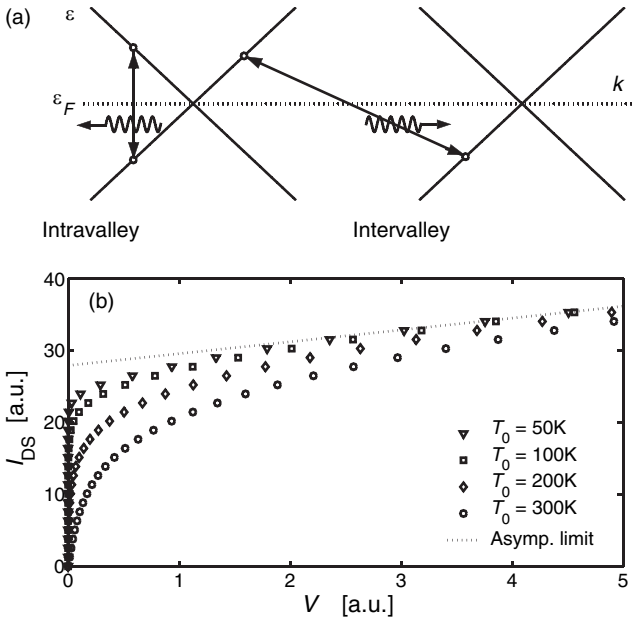

FIG. 1. (a) Scattering processes considered in the calculations. The intravalley (left) and intervalley (right) transitions with emission and absorption of optical phonons are included. (b) *IV* characteristics for different constant temperatures along the tube. Dashed line: asymptotic behavior for all temperatures in the high bias regime.

Fig. 1(a), the different processes (interbranch and intrabranch) considered in $C_{\rm ph}$ include both the emission and absorption of these phonons with energy ($\hbar\omega_{\rm op} \approx 0.2$ eV) much larger than thermal fluctuations at room temperature. Each of these phonons contributes to the collision integral as follows:

$$C^{\alpha}_{\rm ph}(I, T(x)) = \sum_{i,\beta}\Big\{\frac{R^i_e}{\pi}\{f^{\beta}(k)[1 - f^{\alpha}(k-q)] - f^{\alpha}(k)[1 - f^{\beta}(k-q)]\} + \frac{R^i_a}{\pi}\{f^{\beta}(k)[1 - f^{\alpha}(k+q)] - f^{\alpha}(k)[1 - f^{\beta}(k+q)]\}\Big\}, \quad (3)$$

where the index β runs over the two branches and two valleys, i stands for OP and ZB phonons, and R^i_e (R^i_a) is the phonon emission (absorption) rate. Hence the first (second) two terms in Eq. (3) correspond to processes involving the emission (absorption) of a phonon limited by Pauli exclusion principle. For instance, the first term describes a process in which an electron scatters from a state in branch β with momentum k to a state in branch α with momentum $k - q$ by emitting a phonon. In all these processes both total energy and momentum are conserved. The emission and absorption rate coefficients are given by

$$R^i_a(T_L) = \frac{N_q}{\tau_i} = \frac{1}{\tau_i}\frac{1}{\exp(\hbar\omega/k_B T_L) - 1}, \quad (4)$$

$$R^i_e(T_L) = \frac{N_q + 1}{\tau_i} = R_a \exp(\hbar\omega/k_B T_L), \quad (5)$$

where T_L is the lattice temperature and $1/\tau_i$ stands for the bare scattering rate for OP and ZB phonons that we assume to be independent of carrier energy in a first approximation. In computing the collision integral, we make the key "ansatz" that electrons and lattice are in local thermal equilibrium [i.e., $T_L = T_L(x) = T_{\rm el}(x)$] [13]. We define the electron density as

$$n_{\alpha} = \frac{1}{\pi}\int_{-k(E_c)}^{+\infty} f^{\alpha}(k)dk, \quad (6)$$

where E_c is the bottom of the conduction band, and the current as

$$I = e(n_+ - n_-)v_F, \quad (7)$$

where the + (−) index corresponds to the branches with positive (negative) Fermi velocity. Then, integrating Eq. (1) over the momentum for each branch, and properly accounting for different branches, we obtain

$$v_F \partial_x (n^+ - n^-) = 0, \quad (8)$$

$$v_F \partial_x (n^+ + n^-) - \frac{2eF}{\pi\hbar} = 2\int dk C_{\rm ph}(I, T(x)) = 2\tilde{C}_{\rm ph}(I, T(x)). \quad (9)$$

Equation (8) is the expression of the current conservation in the system, in which by symmetry $\epsilon^{+}_{F1} = \epsilon^{+}_{F2}$ and with charge neutrality in the CN yields $\epsilon^{+}_{F(1,2)} = -\epsilon^{-}_{F(1,2)}$. Integrating Eq. (9) over the length of the nanotube L and assuming equal electron densities at the contacts, we find the voltage drop $V_{\rm DS}$ along the nanotube to be

$$V_{\rm DS} = -\frac{\pi\hbar}{e}\int_{-L/2}^{L/2} dx \tilde{C}_{\rm ph}(I, T(x)). \quad (10)$$

This equation implicitly depends on the current and the temperature profile along the nanotube. In order to obtain both of these quantities, the equation must be solved self-consistently with the heat transport equation.

As a particular case, it is interesting to compute the *IV* relation from Eq. (10) by assuming only OP phonon scattering at constant temperature [i.e., $T(x) = T_0$] in the CN. The results are plotted in Fig. 1(b), where the high bias regime exhibits an asymptotic behavior independent of temperature which is given by

$$V_{\rm DS}(I) = \frac{1}{G_0}\frac{L}{v_F \tau_{\rm op}}(I - I_{\omega_{\rm op}}), \quad (11)$$

where $I_{\omega_{\rm op}} = e\omega_{\rm op}/\pi$ is the threshold current corresponding to the onset of electron backscattering by OP phonons [4], and $G_0 = 2e^2/h$ is the quantum conductance. We should point out that Eq. (11) is not consistent with the current interpretation of electrons accelerated ballistically in the electric field until acquiring enough energy to emit a

phonon, but rather results from the imbalance between the population of the energy branches with positive and negative Fermi velocities. When considering also ZB phonons, the voltage drop in the m-SWNT is a linear combination of expressions similar to Eq. (11), and it still results in a threshold current, only with a more complicated expression.

When heating effects become relevant, thermal dissipation is taken into account self-consistently with Eq. (10). We consider two mechanisms for heat dissipation: (i) diffusion through the supporting substrate (if the CN stands on one) and (ii) flow through the contacts. Hence, by defining $\Delta T = T(x) - T_0$ (where T_0 is the temperature of the substrate and leads), the heat equation becomes [14]

$$-\kappa \frac{d^2 \Delta T}{dx^2} + \gamma \Delta T = q^*, \tag{12}$$

where κ is the thermal conductivity, γ is the coupling coefficient with the substrate, and q^* is the power dissipated per unit volume. Here we make the usual approximation that process (i) is proportional to the local temperature difference between CN and substrate. In our calculations both the thermal conductivity and the coupling coefficient are assumed to remain constant along the tube. The coefficient γ is given [14] by $\gamma = \kappa_{\rm sub}/(td)$, where $\kappa_{\rm sub}$, t, and d are the thermal conductivity of the substrate, the diameter of the nanotube, and the thickness of substrate, respectively. We also assume that the power is homogeneously generated along the CN and given by Joule's law:

$$q^* = jF, \tag{13}$$

where $j = I/A$ is current density through the effective cross section A and the electric field F is given by $F = |V_{\rm DS}/L|$. Then the solution for the temperature profile is given by

$$\Delta T(x) = \frac{q^*}{\gamma L S}\left[1 - \frac{\cosh(\Gamma x)}{\cosh(\Gamma L/2)}\right], \tag{14}$$

where $\Gamma = \sqrt{\gamma/\kappa}$.

Different scenarios can take place depending on the value ΓL (see the inset of Fig. 2). On the one hand, diffusion through the substrate is negligible for $\Gamma L \ll 1$ and the temperature profile exhibits a parabolic shape. On the other hand, for $\Gamma L \gg 1$, heat basically dissipates through the substrate and the temperature is almost constant along the CN. This latter situation occurs in long tubes strongly coupled to the substrate. In all cases, the highest temperature point is at the middle of the tube.

In our calculations we use $T_0 = 300$ K. The energies of OP and ZB phonons are $\hbar\omega_{\rm op} = 0.20$ eV and $\hbar\omega_{\rm zb} = 0.16$ eV, respectively. We use the standard accepted value for the thermal conductivity κ (30 W/cmK) [15] and $\gamma = 10^{11}$ W cm^{-3} K^{-1}. Figure 2 shows the temperature difference in the middle of the tube [$\Delta T(0)$] as a function of I for different CN lengths, corresponding to the data of Ref. [5].

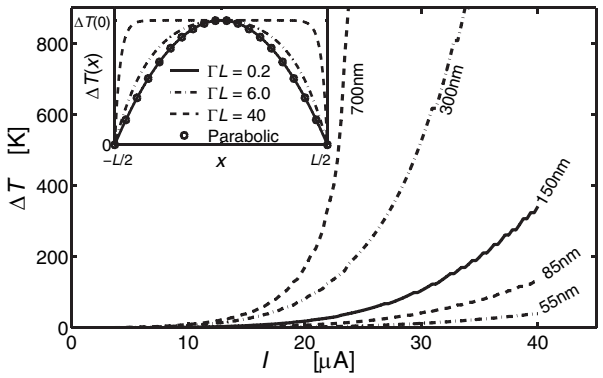

FIG. 2. Temperature difference between the middle of the tube and the leads as a function of the current for different CN lengths [5]. Inset: temperature profile along the NT for different values of ΓL.

The longer the nanotube, the faster the rise in temperature as the threshold current is overcome. This is due to the fact that dissipation occurs over a longer distance while heat removal mainly takes place at the contacts in 1D structures. Estimates for the breakdown temperature correspond to 800 °C [16]. Therefore short tubes are expected to carry larger currents before thermal breakdown. As shown in Fig. 3, the results for the IV characteristics are in good agreement with the experimental data [5,6]. Deviations in the low bias regime are mainly due to the absence of acoustic phonon scattering in our model. For the sake of simplicity, we assume relaxation times for OP and ZB phonons with equal values, which are $\tau = (13 \pm 2)$ fs for the first [5] and $\tau = (6.9 \pm 1.5)$ fs for the second [6] set of experimental data. The difference between the two values could be due to the fact that CNs may have different diameters with different phonon spectra (breathing modes) [17] in each case and contact quality. Nevertheless, the obtained mean free paths (between 6 and 10 nm) are

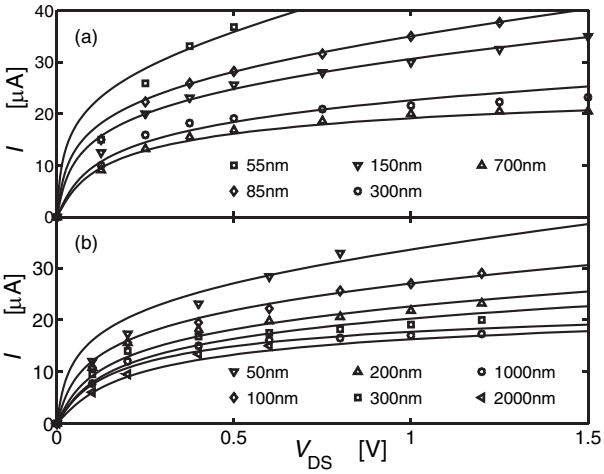

FIG. 3. Comparison between theoretical and experimental IV characteristics for different CN lengths: (a) Ref. [5] and (b) Ref. [6].

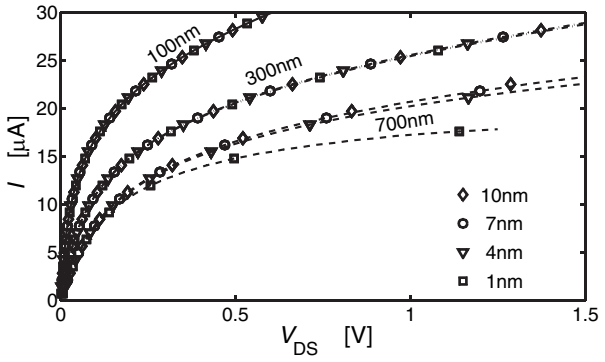

FIG. 4. *IV* characteristics for different tube lengths and diameters. Results are practically independent of the diameter for short tubes (100 and 300 nm); appreciable deviations appear for the smallest diameter (1 nm) in the 700 nm tube.

consistent with previous experimental estimates [5,6]. For long tubes (i.e., for $L = 700$ nm in the first case [5] and for $L \geq 1000$ nm in the second case [6]) we need to increase the relaxation times to (27 ± 3) fs to fit the experimental data. Since at the same current level, the temperature is considerably higher in long CNs, these longer times may be associated with the emergence of nonlinear thermal effects not taken into account in Eq. (12), or to the temperature and geometry dependence of the thermal conductivity at room temperature or higher in *m*-SWNTs, which remains an open issue [18,19].

Finally, Fig. 4 shows the *IV* characteristics obtained for CNs of different diameters and lengths, assuming that both the thermal conductivity and the relaxation time are equal among tubes. Despite this strong assumption, the relevant issue to emphasize here is the weak dependence of the *IV* characteristics on the size of the CN. Appreciable deviations can be observed only in the 700 nm tube (dashed line) for small diameters ($\sim$1 nm). This weak relation is consistent with the interpretation of Collins *et al.* [7,8] for the breakdown under electrical stress observed in MWNTs, where different layers in a MWNT (separated by about 0.4 nm) carry similar currents in the high bias regime. The breakdown of successive carbon layers produces approximately constant diminutions of the current in the high bias regime because *IV* characteristics are geometry independent. Moreover, the highest temperature arises at the CN midlength (inset of Fig. 2) and therefore electrical breakdown is, as experimentally observed, expected to take place there as well.

In conclusion, we have shown that the consideration of a thermalized electron distribution in local equilibrium with a nonhomogeneously heated lattice through OP and ZB scattering determined self-consistently by the current level accounts for the nonlinear *IV* characteristics of the *m*-SWNTs in the high bias regime. The magnitude of the temperature variation as a function of the CN length is consistent with the occurrence of thermal breakdown at midlength for long CN under electrical stress. While the dependence of thermal conductivity on temperature still remains under investigation, our self-consistent model provides a coherent picture of the onset of thermal effects with electronic transport in *m*-SWNT.

The authors are indebted to E. Pop and H. Dai for technical comments. This work was supported by the Beckman Institute for Advance Science and Technology and NSF-Network of Computational Nanotechnology.

[1] R. Saito, G. Dresselhaus, and M. Dresselhaus, *Physical Properties of Carbon Nanotubes* (Imperial College Press, London, 1998).
[2] P. L. McEuen, M. S. Fuhrer, and H. Park, IEEE Trans. Nanotechnol. **1**, 78 (2002).
[3] Ph. Avouris, J. Appenzeller, R. Martel, and S. Wind, Proc. IEEE **91**, 1772 (2003).
[4] Z. Yao, C. L. Kane, and C. Dekker, Phys. Rev. Lett. **84**, 2941 (2000).
[5] A. Javey, J. Guo, M. Paulsson, Q. Wang, D. Mann, M. Lundstrom, and H. Dai, Phys. Rev. Lett. **92**, 106804 (2004).
[6] J. Y. Park, S. Rosenblatt, Y. Yaish, V. Sazonova, H. Üstünel, S. Braig, T. A. Arias, P. W. Brouwer, and P. L. McEuen, Nano Lett. **4**, 517 (2004).
[7] P. G. Collins, M. Hersam, M. Arnold, R. Martel, and Ph. Avouris, Phys. Rev. Lett. **86**, 3128 (2001).
[8] P. G. Collins, M. S. Arnold, and P. Avouris, Science **292**, 706 (2001).
[9] R. S. Muller and T. I. Kamins, *Device Electronics for Integrated Circuits* (John Wiley & Sons, New York, 2002), 3rd ed.
[10] R. A. Jishi, D. Inomata, K. Nakao, M. S. Dresselhaus, and G. Dresselhaus, J. Phys. Soc. Jpn. **63**, 2252 (1994).
[11] R. Saito, T. Takeya, T. Kimura, G. Dresselhaus, and M. S. Dresselhaus, Phys. Rev. B **57**, 4145 (1998).
[12] V. Perebeinos, J. Tersoff, and Ph. Avouris, Phys. Rev. Lett. **94**, 027402 (2005).
[13] This ansatz is relatively satisfied here as the temperature gradient is not very important because, as shown in Fig. 2, in short CNs the temperature does not increase as drastically with current as in long CNs, and for the latter the temperature profile is relatively flat except at the edge, with minor consequences.
[14] C. Durkan, M. A. Schneider, and M. E. Welland, J. Appl. Phys. **86**, 1280 (1999).
[15] J. Che, T. Cagin, and W. A. Goddard III, Nanotechnology **11**, 65 (2000).
[16] M. Radosavljevic, J. Lefebvre, and A. T. Johnson, Phys. Rev. B **64**, 241307 (2001).
[17] B. J. LeRoy, S. G. Lemay, J. Kong, and C. Dekker, Nature (London) **432**, 371 (2004).
[18] T. Yamamoto, S. Watanabe, and K. Watanabe, Phys. Rev. Lett. **92**, 075502 (2004).
[19] J. X. Cao, X. H. Yan, Y. Xiao, and J. W. Ding, Phys. Rev. B **69**, 073407 (2004).